ESTIMATION OF WINTER WHEAT SPAD VALUES USING OPTIMISED FEATURE SELECTION AND MACHINE LEARNING
/
基于优化特征优选和机器学习的冬小麦 SPAD 值估算

Susu HUANG[1)], Junke ZHU[*1,2,4)], Yubin LAN[1,3)], Ning YANG[2)], Yan SUN[4)], Yijing LIANG[1)], Zhenxin LIANG[1)], Yuxin ZHU[5)], Yuwei FU[1)]

[1)]Shandong University of Technology, School of Agricultural Engineering and Food Science, Zibo / China;
[2)] Qilu Normal University, School of Life Sciences, Jinan / China;
[3)]National Sub-Centre for International Collaboration Research Centre for Agricultural Aviation Intelligent Equipment, Zibo / China
[4)]Zibo Hefeng Seed Technology Co., Ltd., Zibo / China;
[5)]Shandong Agricultural University, College of Economics and Management, Tai'an / China;
Tel: +8618905338833; E-mail: zhujunke@126.com
Corresponding author: Junke ZHU
DOI: https://doi.org/10.35633/inmateh-77-64

Keywords: *Winter wheat, SPAD values, UAV remote sensing, spectral characteristics, feature selection, machine learning*

ABSTRACT
To achieve high-precision non-destructive monitoring of SPAD values in winter wheat, this study proposes an estimation method integrating multi-feature optimization with machine learning. Based on UAV multispectral imagery and synchronous ground measurement data from 33 plots, the research was conducted during three critical growth stages: jointing, heading, and grain filling. The PCC-RF-CV method was employed for feature fusion and optimization, identifying optimal feature combinations for each stage from multiple vegetation indices and texture features. Six machine learning models were constructed for comparison. Results indicate: the multi-source feature fusion strategy demonstrated superior performance throughout all growth stages; PCC-RF-CV effectively optimized feature inputs, establishing optimal feature sets for each stage; The XGBoost model developed for the grain filling stage achieved the best estimation performance (validation set R^2 = 0.92, RMSE = 0.36, MAE = 0.30). This study provides a reliable method for accurately estimating SPAD values in winter wheat and analyzing canopy spectral dynamics, offering robust technical support for crop growth monitoring and precision agriculture.

摘要
为实现冬小麦 SPAD 值的高精度无损监测，本研究提出一种融合多特征优选与机器学习的估算方法。研究基于 33 个小区的无人机多光谱影像及同步地面测量数据，在拔节、抽穗和灌浆三个关键生育期展开。采用 PCC-RF-CV 方法进行特征融合与优选，从多个植被指数和纹理特征中确定每个时期的最佳特征组合，并构建了六种机器学习模型进行对比。结果表明：多源特征融合策略在全生育期均表现优越；PCC-RF-CV 有效优化了特征输入，为各时期构建了最优特征集；基于此构建的灌浆期 XGBoost 模型估算效果最佳（验证集 R^2 = 0.92, RMSE = 0.36, MAE = 0.30）。本研究为精准估算冬小麦 SPAD 值、解析冠层光谱动态规律提供了可靠方法，为作物生长监测与精准农业提供可靠技术支撑。

INTRODUCTION
Food security is a cornerstone of national strategy *(Wang et al., 2025)*, and winter wheat, as one of the world's major food crops, directly impacts the stability of grain supply through its growth status and yield *(Peng et al., 2024)*. Chlorophyll content serves as a core indicator of crop photosynthetic capacity, typically represented by SPAD values. This parameter is a key physiological indicator for characterizing relative chlorophyll content and assessing plant nitrogen nutrition and growth status *(Xin et al., 2021)*. In recent years, unmanned aerial vehicle (UAV) remote sensing technology has emerged as a vital tool for rapid, non-destructive crop growth monitoring, leveraging its high spatio-temporal resolution and flexibility. By integrating multispectral and RGB images, the non-destructive estimation of multiple photosynthetic indicators of winter wheat and the screening of high photosynthetic efficiency varieties have been successfully achieved, verifying the feasibility of this technology in intelligent breeding *(Feng et al., 2024)*.

In the estimation of remote sensing parameters, feature selection is a key step in building high-precision and robust predictive models, especially in the context of multi-source remote sensing feature fusion, where it plays a more prominent role in eliminating redundant information and identifying key variables. In the study of winter wheat, feature fusion and selection can achieve precise classification of frost damage levels *(Zhu et al., 2025)*, with an XGBoost model accuracy of 0.73 and an F1 score of 0.69, significantly enhancing the discriminative ability of the model; while using competitive adaptive re-weighted sampling for feature extraction can effectively improve the accuracy and robustness of the leaf water content prediction model *(Zhao et al., 2022)*. The value of feature selection is particularly prominent in the framework of multi-source feature fusion. For example, feature optimization using decision trees can significantly improve the estimation accuracy of citrus SPAD and leaf water content *(Liu et al., 2025)*; likewise, screening key variables by fusing optical and microwave remote sensing features through random forest importance scores has been proven to effectively construct a high-performance leaf area index estimation model for yellow chrysanthemum *(Hu et al., 2025)*.

Nevertheless, existing feature selection methods *(Su et al., 2024)* exhibit significant limitations when applied to SPAD value estimation for winter wheat across multiple growth stages. First, the comprehensiveness of the feature selection strategy is insufficient. Most studies adopt a single method, which is unable to simultaneously capture the complex linear and non-linear relationships between features and the target (*Ma et al., 2025*). Moreover, when determining the final feature set, it is highly subjective and lacks an objective optimization process (*Nigon et al., 2020*). Secondly, the adaptability to the dynamic characteristics of the growth period is insufficient. The crown structure and physiological characteristics of winter wheat change dynamically with the growth process (*Zhang et al., 2024*), and the association mechanism between its features and SPAD values also changes accordingly. However, most current feature selection methods adopt a static design and fail to reflect this specificity (*Wu et al., 2025*).

In response to the above issues, this study selected winter wheat from the ecological unmanned farm of Shandong University of Technology as the research object. Based on multi-spectral images from unmanned aerial vehicles, three feature selection strategies, namely PCC, RF-CV, and PCC-RF-CV, were systematically constructed and compared. Combined with six machine learning algorithms, including support vector regression (SVR), extreme gradient boosting (XGBoost), error backpropagation neural network (BPNN), K-nearest neighbor (KNN), partial least squares regression (PLSR), and multiple linear regression (MLR), the performance of different feature selection methods combined with various modeling algorithms in estimating SPAD values during multiple growth stages was comprehensively evaluated. Finally, a spatiotemporal distribution map of SPAD values was generated based on the optimal estimation model, with the aim of providing reliable method support for precise nitrogen nutrition monitoring and intelligent agricultural management of winter wheat.

MATERIALS AND METHODS

Study area overview

The experimental site for this study is located at the Shandong University of Technology Ecological Unmanned Farm in Zibo City, Shandong Province (36°57'5"N, 118°13'16"E).

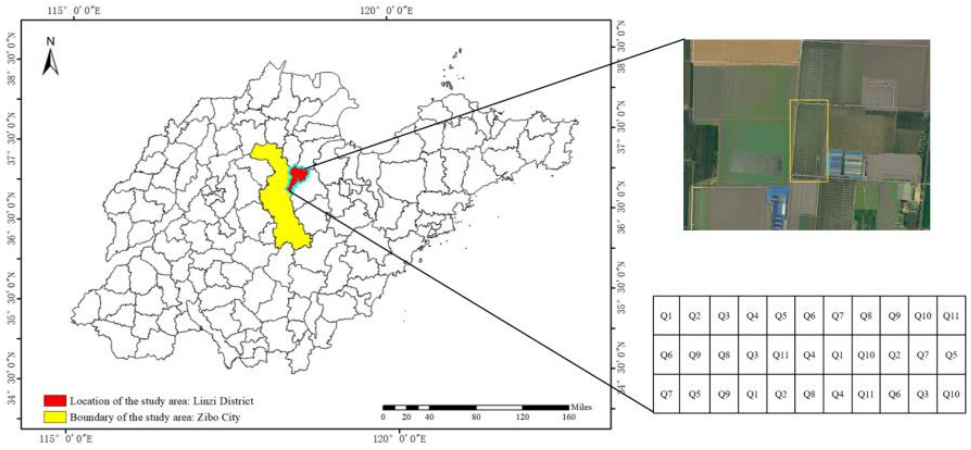

Fig. 1 - Overview of the test area

This area represents a typical plain region with a temperate semi-humid semi-arid continental climate, featuring annual average sunshine hours of 2100–2500 hours, an average temperature of 13.2°C, and annual precipitation of 650–800 mm. Data collection occurred during winter wheat's jointing stage (April 2), heading stage (April 26), and grain filling stage (May 15). A randomized block design was employed, comprising 11 varieties (lines) with 3 replications, totaling 33 experimental plots measuring 9 m × 1.5 m each.

Data acquisition and processing

This study employed a DJI M3M drone platform to simultaneously collect remote sensing data and ground SPAD values. Equipped with visible and multispectral cameras, the drone captured imagery during three critical growth stages of winter wheat under clear weather conditions between 10:00 and 14:00. Flight altitude was maintained at 30 meters, with 80% overlap in both forward and sideways directions. SPAD values were measured using a SPAD-502Plus chlorophyll meter at five sampling points.

Image data underwent orthorectification and other preprocessing in Pix4D Mapper. Radiometric calibration and NDVI threshold segmentation were performed in ENVI 5.6 to eliminate soil background. Vegetation indices were calculated and texture features extracted across 33 delineated plots. Average values of effective vegetation pixel characteristics were statistically derived for each plot as modeling inputs. All data processing and analysis were conducted in a Python 3.11 environment.

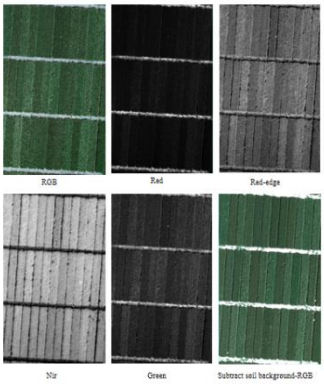

Fig. 2 - Multispectral band reflectance characteristics and soil background removal

SPAD values of winter wheat in the field

The statistical characteristics of SPAD values during the three growth stages of winter wheat are shown in Table 1. The data indicate that SPAD values exhibit a trend of initially decreasing and then increasing, reflecting enhanced photosynthetic function during the grain filling stage. Data stability was high across all stages (coefficient of variation<5%), with the lowest variation occurring during grain filling. Significant individual variation was observed during the early growth stage, which tended to converge later on. This pattern provides reliable evidence for leaf physiological monitoring.

Table 1

Statistical data of SPAD values for winter wheat

Growth stage	Sample size	Maximum value	Minimum value	Average value	Standard deviation	Variance	Coefficient of Variation
Jointing stage	33	63.97	53.28	57.74	2.35	5.5	4.06%
Heading stage	33	60.21	53.17	57.35	2.18	4.73	3.79%
Filling stage	33	64.72	57.68	60.68	1.7	2.88	2.80%

Selection of spectral features

In the SPAD value estimation of winter wheat, spectral feature optimization is crucial. This study constructed a feature set comprising 50 spectral characteristics based on vegetation spectral properties. This set includes 9 RGB vegetation indices, 9 multispectral vegetation indices, and 32 texture features.

Through mathematical combination, this feature set enhances vegetation information while suppressing background noise. Its multidimensional structure effectively characterizes canopy biochemical and structural properties (*Sun et al., 2025*), laying the foundation for improving SPAD value estimation accuracy.

Feature selection methods

To achieve high-precision estimation of SPAD values for winter wheat, it is necessary to select feature combinations with high sensitivity and low redundancy from multidimensional characteristics. This study systematically compared three feature selection methods to evaluate the applicability and effectiveness of different strategies across various growth stages of winter wheat.

Pearson correlation coefficient (PCC)

This method measures the strength of linear correlation by calculating the Pearson correlation coefficient (r) between each feature and the SPAD value (*Guo et al., 2025*). The range of r is $[-1, 1]$. A higher absolute value closer to 1 indicates stronger correlation. When PCC is employed as an independent feature selection method, this study utilizes a higher threshold ($|r|>0.7$) for screening. This threshold is based on the statistical criterion for strong correlation (*Liu et al., 2023*), aiming to obtain the feature subset most significantly linearly correlated with SPAD values to construct a concise and efficient estimation model.

Random forest with cross validation (RF-CV)

Random forests evaluate feature contributions by calculating the average reduction in impurity during decision tree node splitting (*Yang et al., 2024*). Feature importance scores are computed based on out-of-bag error, where higher importance indicates greater influence on SPAD value estimation. Combining 10-fold cross-validation with grid search and using RMSE as the evaluation metric, the optimal number of features for each growth stage is determined.

Feature fusion optimization method (PCC-RF-CV)

To overcome the limitations of using either PCC or RF-CV alone, this study proposes a two-stage feature fusion optimization strategy combining PCC and RF-CV. This method employs PCC for linear pre-filtering, followed by RF-CV for nonlinear fine-tuning, achieving effective complementarity and coupling between the two approaches. The overall workflow of this strategy, illustrated in Figure 3, comprises two core stages: linear pre-dimension reduction and nonlinear fine-tuning. The specific steps are as follows:

(1) Feature Input and PCC Preliminary Screening: All 50 original spectral features are input into the screening process. Initial linear screening is performed using Pearson's correlation coefficient to rapidly eliminate features with negligible correlation to SPAD values while retaining a subset of potentially relevant features. Setting a threshold $|r|$ >0.5 reduces computational complexity in subsequent steps.

(2) RF Importance Ranking: The feature subset post-PCC screening is input into a Random Forest regression model for training. Feature importance scores are calculated based on out-of-bag error, then ranked in descending order to establish a feature importance sequence.

(3) CV Determination of Optimal Feature Count: Employ ten-fold cross-validation with root mean square error (RMSE) as the evaluation metric to systematically assess model performance from the first to the Nth feature. Grid search identifies the feature count K that minimizes RMSE, establishing it as the optimal feature count for this growth stage.

(4) Final Feature Combination Output: Based on the determined optimal feature count K, select the top K features from the feature importance sequence to form the optimal feature combination for final modeling, completing the two-stage feature selection process.

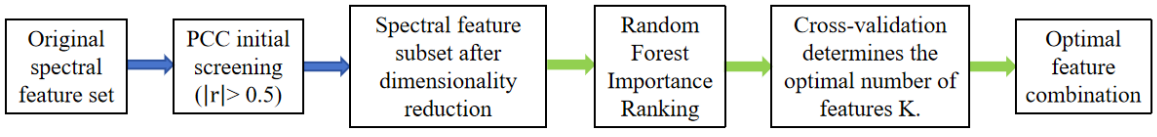

Fig. 3 - Flowchart of the PCC-RF-CV feature selection algorithm

Machine learning models and evaluation metrics

This study utilized drone remote sensing data and ground-measured SPAD values from three critical growth stages of winter wheat. The dataset was divided into training and validation sets at a 7:3 ratio. Six machine learning estimation models were constructed using Python programming language. The fundamental principles and key parameter settings for each algorithm are presented in Table 2.

Model performance evaluation employed three metrics: the coefficient of determination (R^2), root mean square error (RMSE), and mean absolute error (MAE). Comprehensive analysis of these metrics enabled a holistic assessment of each model's performance in winter wheat chlorophyll content estimation, thereby identifying the optimal estimation model.

Table 2

Machine learning algorithm configuration specifications

Algorithm Name	Core principle	Implementation tool	Key parameter settings
SVR	Finding the optimal hyperplane to minimize sample distance	scikit-learn	Nuclear function: linear ; C: 0.1
XGBoost	Gradient boosting decision trees, iterative residual fitting	xgboost	n_estimators=100； learning_rate=0.01
BPNN	Error backpropagation adjusts weights	scikit-learn	Hidden layers: 2 layers; Optimizer: SGD; Learning rate: 0.01
KNN	Nearest neighbor sample mean prediction	scikit-learn	Distance metric: Euclidean distance; K value: 3–15
PLSR	Principal component analysis to overcome multicollinearity	scikit-learn	Number of principal components: determined by cross-validation
MLR	Least squares estimation of regression coefficients	scikit-learn	No special parameter settings

RESULTS AND ANALYSIS

Comparison of results from different feature selection methods

This study systematically compared three strategies—PCC, RF-CV, and PCC-RF-CV—aiming to establish a foundation for subsequent high-precision prediction models by selecting optimal features from a candidate set comprising RGB, multispectral vegetation indices, and texture features.

Feature selection results based on PCC

Results based on Pearson correlation coefficient (PCC) analysis indicate that the strength of association between spectral features and SPAD values dynamically changes throughout the growth stages. As shown in Figure 4, the NDRE index maintained the highest correlation across all growth stages, demonstrating a stable response to chlorophyll content. Correlations for other indices exhibited significant fluctuations, reflecting the pronounced influence of canopy physiological changes on spectral responses. This study set $|r|>$ 0.7 as the threshold. The optimal feature combinations selected for each growth stage are presented in Table 3.

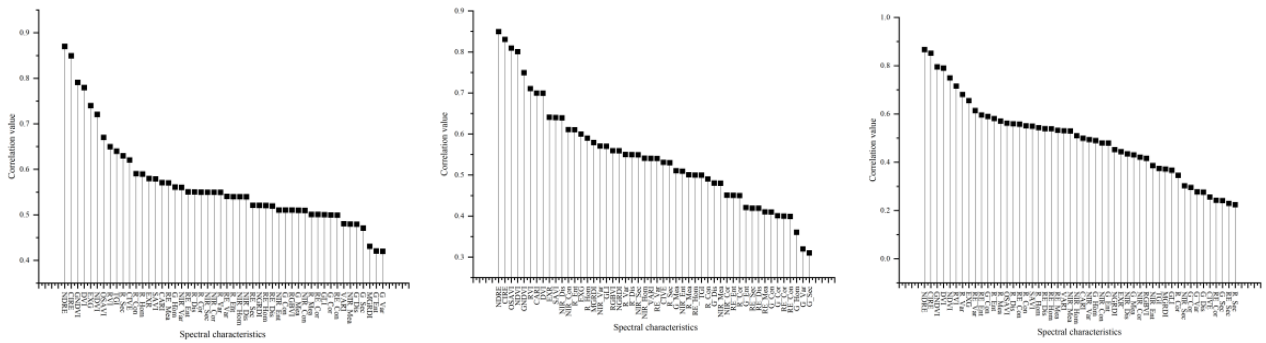

(a) Jointing stage *(b) Heading stage* *(c) Filling stage*

Fig. 4 - Ranking of spectral features based on PCC correlation with SPAD values

Table 3

Spectral feature selection results for each growth stage based on PCC

Growth stage	Spectral characteristics
Jointing stage	NDRE, CIRE, GNDVI, DVI, EXG, NDVI
Heading stage	NDRE, CIRE, OSAVI, NDVI, GNDVI, RVI
Filling stage	NDRE, CIRE, GNDVI, DVI, NDVI, RVI

Feature selection results based on RF-CV

Feature selection results based on the RF-CV method indicate significant differences in the optimal number of features across growth stages. As shown in Figure 5, RMSE reached its minimum values at 6, 9, and 7 features during the jointing, heading, and grain filling stages, respectively, reflecting the intrinsic variations in spectral response mechanisms during different growth phases of winter wheat. The optimal feature combinations for each growth stage are presented in Table 4.

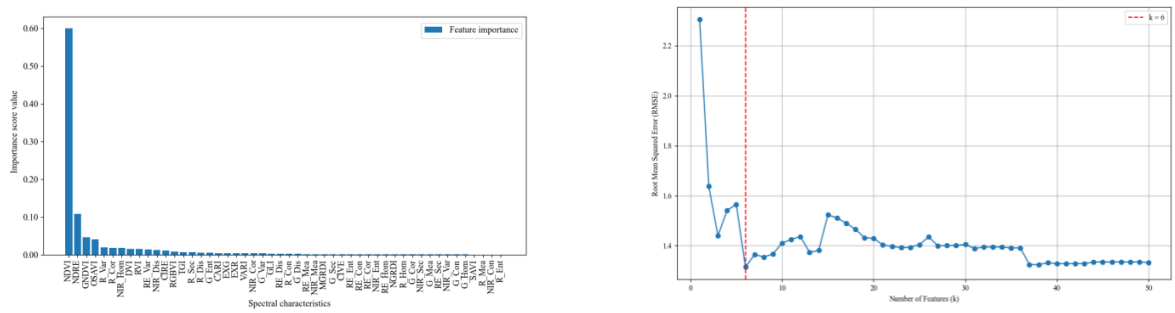

(a) Jointing stage

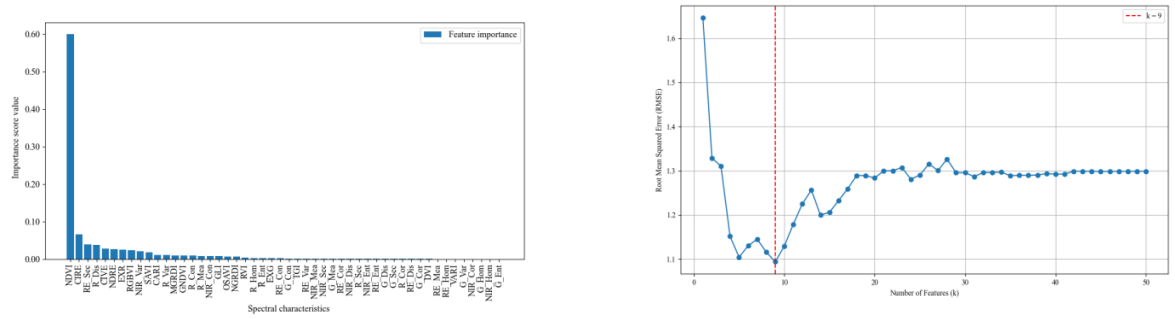

(b) Heading stage

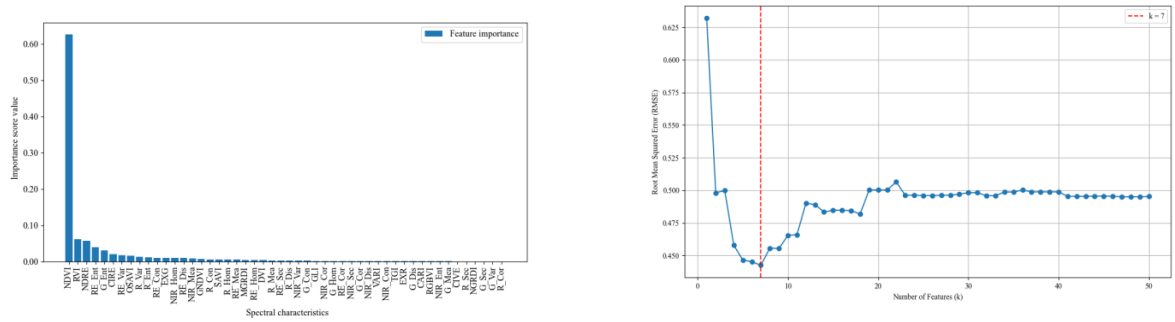

(c) Filling stage

Fig. 5 - Importance scores and cross-validation results for each growth stage based on RF-CV

Table 4

Spectral feature selection results for each period based on RF-CV

Growth stage	Spectral characteristics
Jointing stage	NDVI, GNDVI, NDRE, OSAVI, R_Var, R_Cor
Heading stage	NDVI, CIRE, NDRE, ExR, RGBVI, CIVE, R_Dis, RE_Sec, NIR_Var
Filling stage	NDVI, RVI, CIRE, NDRE, RE_Var, RE_Ent, G_Ent

Feature selection results based on PCC-RF-CV

To integrate the advantages of linear and nonlinear feature selection, this study employed the PCC-RF-CV fusion method for feature optimization. Feature importance rankings and cross-validation results are presented in Figure 6. The results indicate that for both the jointing stage and heading stage, the model RMSE was minimized when 5 features were selected. For the grain filling stage, the RMSE was minimized when 6 features were selected. The optimal feature subsets for each growth stage are shown in Table 5.

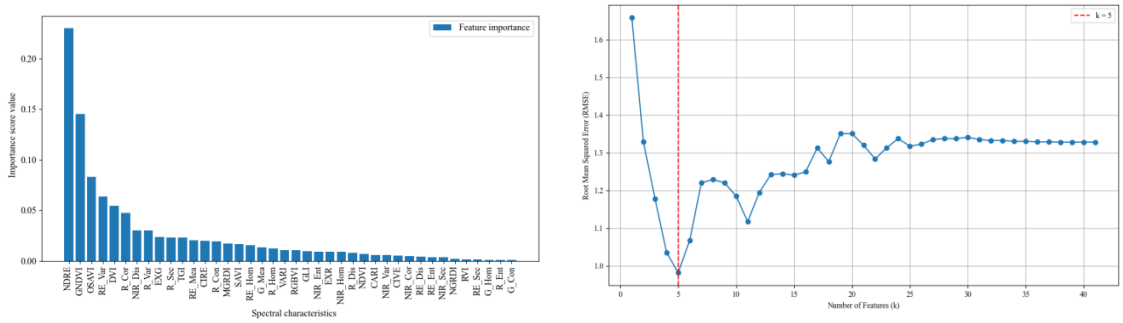

(a) Jointing stage

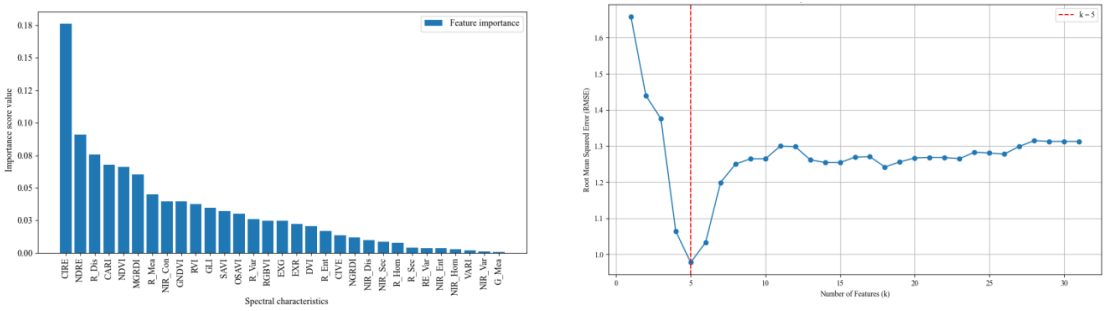

(b) Heading stage

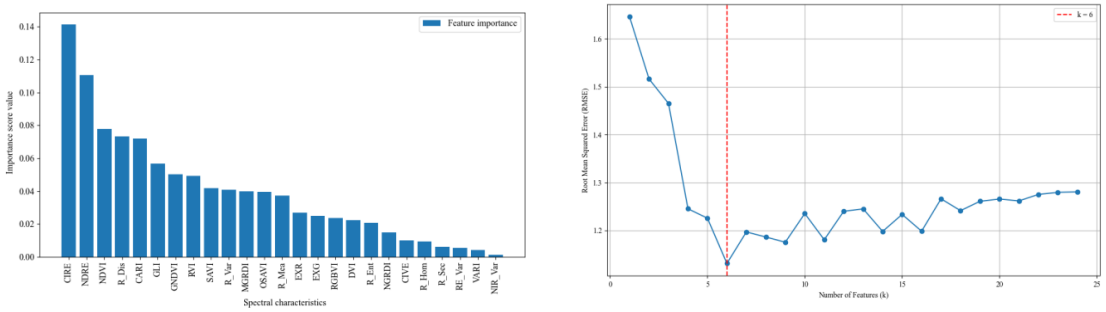

(c) Filling stage

Fig. 6 - Importance scores and cross-validation results for each growth stage based on PCC-RF-CV

Table 5

Spectral feature selection results for each period based on PCC-RF-CV

Growth stage	Spectral characteristics
Jointing stage	NDRE, GNDVI, OSAVI, RE_Var, DVI
Heading stage	CIRE, NDRE, R_Dis, CARI, NDVI
Filling stage	CIRE, NDRE, NDVI, R_Dis, CARI, GLI

Performance evaluation of SPAD value estimation models at different growth stages

To systematically evaluate the performance of different feature selection strategies in estimating SPAD values for winter wheat, this study constructed multi-growth-stage prediction models based on three feature selection methods and six machine learning models. The validation set accuracy evaluation results are detailed in Table 6 and Figure 7.

Comparative analysis of different feature selection methods indicates that the PCC-RF-CV fusion strategy demonstrates significant advantages, particularly during the grain filling stage. Its model achieved an average R^2 of 0.82, representing improvements of 7.3% and 9.7% over PCC and RF-CV, respectively.

The average RMSE was 0.69, reduced by 28% and 27.7% compared to PCC and RF-CV. This advantage stems from its two-stage design: PCC linear screening achieves efficient dimensionality reduction, while RF-CV nonlinear screening delves into complex relationships. This serial fusion strategy effectively overcomes the limitations of individual methods, thereby selecting an optimal feature subset with stronger discriminative power and lower redundancy.

From a growth stage dynamics perspective, optimal model combinations varied across stages, reflecting the dynamic evolution of winter wheat canopy spectral response mechanisms during development. The PCC-RF-CV-PLSR model performed best during the jointing stage (R^2 = 0.83, RMSE = 0.86, MAE = 0.66); The PCC-RF-CV-MLR model achieved the highest accuracy during the heading stage (R^2 = 0.83, RMSE = 0.95, MAE = 0.78); The PCC-RF-CV-XGBoost combination achieved breakthrough results during the grain filling stage (R^2 = 0.92, RMSE = 0.36, MAE = 0.30), with R^2 improvements ranging from 8.24% to 21.4%. This validates the universality of the PCC-RF-CV approach across different growth stages and underscores the necessity of dynamically optimizing features for distinct developmental periods.

Regarding modeling approaches, XGBoost demonstrated optimal performance during grain filling when combined with PCC-RF-CV features (R^2 = 0.92, RMSE = 0.36, MAE = 0.30), outperforming PLSR and MLR by 8.2% and 7.0%, respectively, while reducing RMSE by 35.7% and 29.4%, respectively. This indicates that ensemble learning methods are more suitable for remote sensing monitoring of crop physiological parameters during the mid-to-late growth stages.

In the comparison of machine learning algorithms, the XGBoost algorithm demonstrated the best predictive performance when combined with the PCC-RF-CV feature set during the grain filling stage (R^2 = 0.92, RMSE = 0.36, MAE = 0.30), representing improvements of 8.2% and 7.0% over PLSR and MLR, respectively. The corresponding RMSE reductions were 35.7% and 29.4%. This demonstrates that XGBoost, with its robust nonlinear fitting capability, holds an advantage in estimating crop physiological parameters when confronting the complex canopy structure and physiological processes during the late growth stage.

In summary, the PCC-RF-CV method systematically enhances SPAD value prediction accuracy. Its integration with XGBoost provides a reliable solution for monitoring crops during critical growth stages.

Table 6

SPAD value prediction model results for winter wheat at different growth stages

Growth stage	Model	PCC			RF-CV			PCC-RF-CV		
		R^2	RMSE	MAE	R^2	RMSE	MAE	R^2	RMSE	MAE
Jointing stage	BPNN	0.71	1.99	1.73	0.66	1.40	1.25	0.74	1.2	1.06
	KNN	0.73	1.64	1.43	0.72	1.36	1.27	0.66	1.63	1.52
	SVR	0.75	1.63	1.35	0.73	1.22	0.93	0.73	1.07	0.94
	XGBoost	0.76	1.53	1.32	0.75	1.11	1.10	0.81	0.98	0.87
	PLSR	0.78	1.60	1.45	0.73	1.31	1.22	**0.83**	**0.86**	**0.66**
	MLR	0.79	1.56	1.31	0.76	1.02	0.90	0.8	1.13	0.92
Heading stage	BPNN	0.73	1.34	1.21	0.65	1.53	1.41	0.77	1.55	1.36
	KNN	0.70	1.41	1.35	0.68	1.45	1.39	0.72	1.39	1.11
	SVR	0.75	1.33	1.24	0.78	1.14	0.99	0.81	1.01	0.83
	XGBoost	0.78	1.28	1.09	0.73	1.38	1.26	0.82	0.97	0.73
	PLSR	0.76	1.22	1.14	0.75	1.22	1.05	0.81	0.96	0.82
	MLR	0.77	1.28	1.17	0.70	1.40	1.20	**0.83**	**0.95**	**0.78**
Filling stage	BPNN	0.74	1.00	0.90	0.70	1.24	1.17	0.76	0.87	0.81
	KNN	0.75	0.91	0.81	0.74	0.92	0.83	0.76	1.01	0.93
	SVR	0.75	0.92	0.80	0.76	0.88	0.74	0.79	0.80	0.73
	XGBoost	0.76	1.31	1.11	0.79	0.82	0.73	**0.92**	**0.36**	**0.30**
	PLSR	0.81	0.76	0.64	0.75	0.93	0.81	0.85	0.56	0.46
	MLR	0.79	0.81	0.69	0.76	0.89	0.76	0.86	0.51	0.45

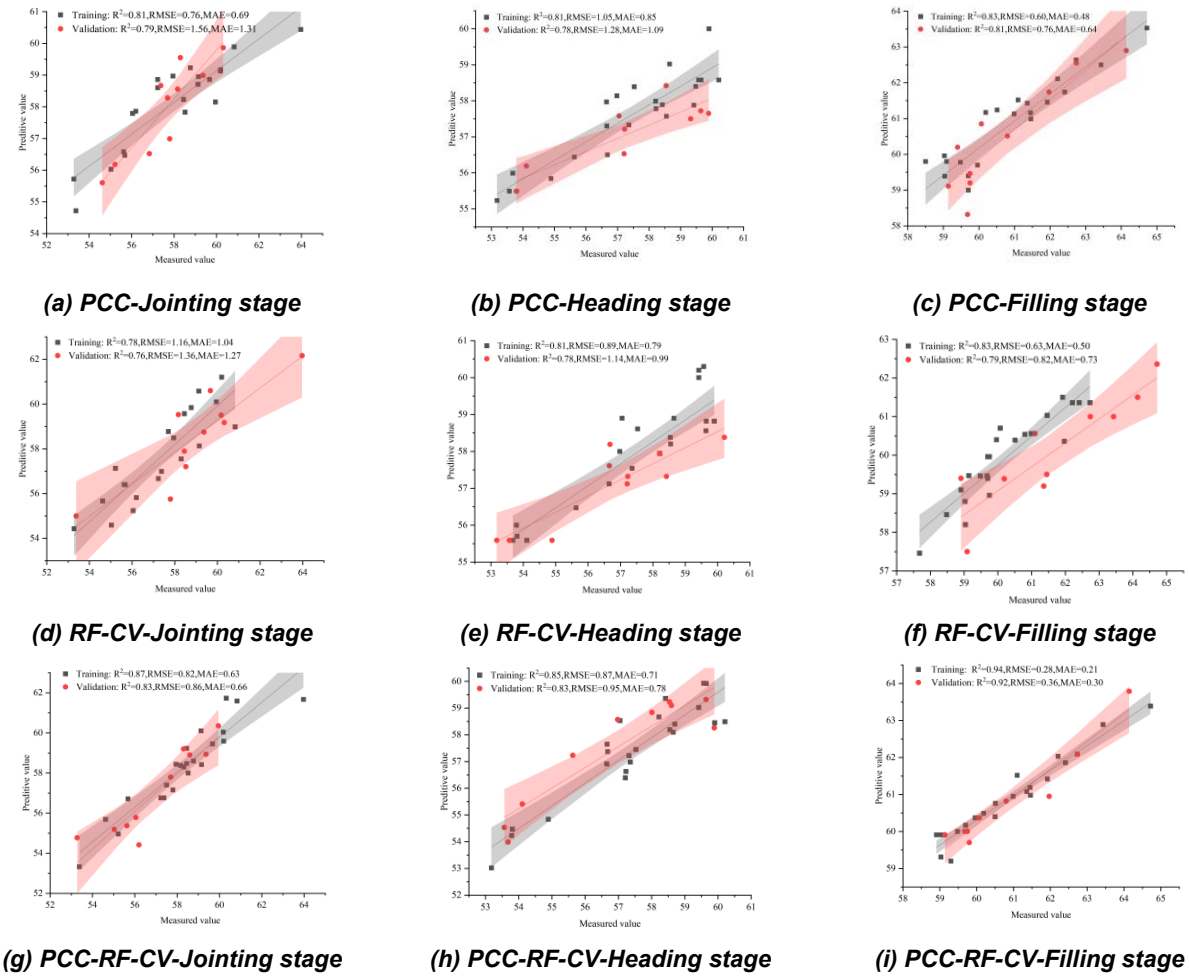

(a) PCC-Jointing stage *(b) PCC-Heading stage* *(c) PCC-Filling stage*

(d) RF-CV-Jointing stage *(e) RF-CV-Heading stage* *(f) RF-CV-Filling stage*

(g) PCC-RF-CV-Jointing stage *(h) PCC-RF-CV-Heading stage* *(i) PCC-RF-CV-Filling stage*

Fig. 7 - Optimal estimation results for SPAD values at different growth stages based on feature selection

Spatio-temporal distribution characteristics of SPAD values based on an optimal model

The spatial distribution of SPAD values generated based on the optimal estimation model is shown in Figure 8. Winter wheat SPAD values exhibit spatiotemporal variation patterns, SPAD values are projected to continue rising from the jointing stage to the grain filling stage, consistent with field measurements, reflecting enhanced photosynthetic function in the later growth stages. SPAD values demonstrate spatial heterogeneity across all stages, with spatial variability significantly decreasing during the grain filling stage, indicating that crop growth trends toward uniformity. These results provide spatial decision-making support for precision agriculture.

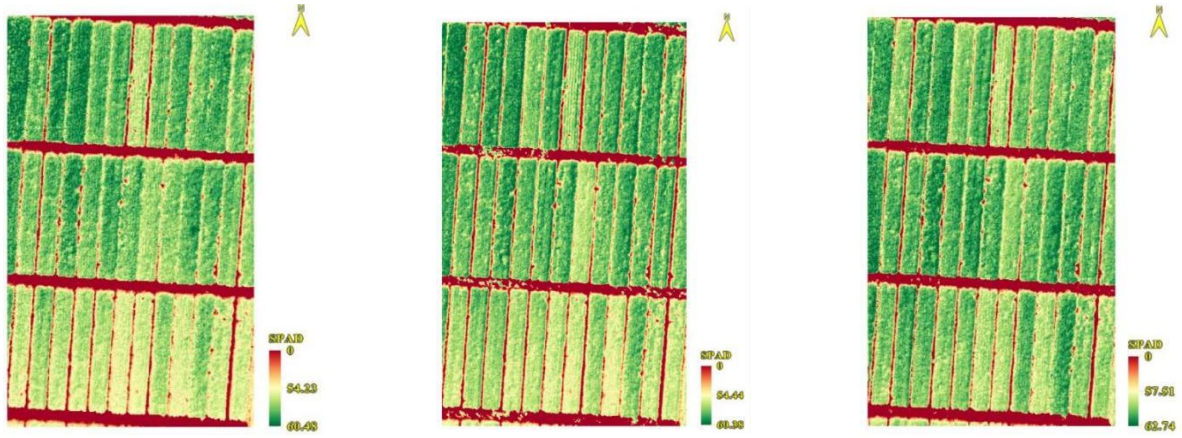

(a) Jointing stage *(b) Heading stage* *(c) Filling stage*

Fig. 8 - Spatiotemporal distribution maps of SPAD values across different periods

CONCLUSIONS

This study proposes a two-stage feature selection method, PCC-RF-CV, that integrates PCC and RF-CV. Previous studies have indicated that relying solely on single feature selection methods for spectral feature screening fails to adequately account for the complementarity and correlation among spectral features (*Wang et al., 2023*). To address this limitation, the proposed method combines PCC linear preliminary screening with RF-CV nonlinear fine screening to determine optimal feature combinations for each growth stage. This approach aims to overcome the aforementioned constraints, significantly enhancing the objectivity of feature selection and the quality of model inputs.

The spectral indices and texture features selected through PCC-RF-CV fusion demonstrated excellent estimation performance across all growth stages of winter wheat. This finding is consistent with the conclusion in the study (*Xian et al., 2024*) regarding the improvement of biomass estimation through multi-feature fusion. It further validates the universality and effectiveness of the collaborative optimization of multiple sources of features in agricultural remote sensing parameter estimation. Among these, the XGBoost model achieved optimal performance during the grain filling stage with R^2=0.92, RMSE=0.36, and MAE=0.30, indicating that multi-feature fusion and dynamic optimization effectively enhance SPAD value estimation accuracy. The conclusion of this study is consistent with the previous findings (*Yang et al., 2025*), and together they prove that the strategy of selecting fused features that fully consider the dynamic of the growth period is an effective way to achieve high-precision estimation of crop SPAD values.

Future research should expand the sample size and integrate additional data sources such as meteorological and hyperspectral information to improve model generalization. This would provide reliable technical support for non-destructive crop growth monitoring in smart agriculture.

ACKNOWLEDGEMENT

This research was supported by the Shandong Provincial Key R&D Program (Agricultural Breeding Project) for the Development and Industrialization of Major New Wheat Varieties with High Yield, Superior Quality, High Efficiency, and Stress Tolerance (2022LZGCQY002).

REFERENCES

[1] Feng, W., Lan, Y., Zhao, H., Tang, Z., Peng, W., Che, H., & Zhu, J. (2024). Identification of High-Photosynthetic-Efficiency Wheat Varieties Based on Multi-Source Remote Sensing from UAVs. *Agronomy*, Vol. 14, pp. 2389-2389, MDPI / Switzerland. https://doi.org/10.3390/AGRONOMY141023 89.

[2] Guo, X., Bayat, B., Bates, J., Herbst, M., Schmidt, M., Vereecken, H., & Montzka, C. (2025). Enhancing carbon flux estimation in a crop growth model by integrating UAS-derived leaf area index. *Agricultural and Forest Meteorology*, Vol. 374, pp. 110776-110776, Elsevier/Netherlands. https://doi.org/10.1016//J.AGRFORMET.2025.110776.

[3] Hu, M., Wang, J., Yang, P., Li, P., He, P., & Bi, R. (2025). Estimation of Daylily Leaf Area Index by Synergy Multispectral and Radar Remote-Sensing Data Based on Machine-Learning Algorithm. *Agronomy*, Vol. 15, pp. 456-456, MDPI / Switzerland. https://doi.org/10.3390/AGRONOMY15020456.

[4] Liu, Q., Chen, F., Cui, N., Wu, Z., Jin, X., Zhu, S., & Wang, Z. (2025). Inversion of citrus SPAD value and leaf water content by combining feature selection and ensemble learning algorithm using UAV remote sensing images. *Agricultural Water Management*, Vol. 314, pp. 109524-109524, Elsevier / Netherlands. https://doi.org/10.1016/J.AGWAT.2025.109524.

[5] Liu, D., & Yan, Y. (2023). Correlation and Causality in Big Data Analysis (大数据分析中的相关性和因果关系). *Journal of National Prosecutors College*, Vol. 31, pp. 23-41, Beijing / China.

[6] Ma, W., Han, W., Cui, X., Zhang, H., Zhang, L., Dong, Y., & Zhai, X. (2025). Soil salinity estimation incorporating environmental covariables using UAV remote sensing for precision field management. *Computers and Electronics in Agriculture*, Vol. 237, pp. 110532-110532, Elsevier / England. https://doi.org/10.1016/J.COMPAG.2025.110532.

[7] Nigon, J T., Yang, C., Paiao, D G., Mulla, J D., Knight, F J., & Fernández, G F. (2020). Prediction of Early Season Nitrogen Uptake in Maize Using High-Resolution Aerial Hyperspectral Imagery. *Remote Sensing*, Vol. 12, pp. 1234-1234, MDPI / Switzerland. https://doi.org/10.3390/rs12081234.

[8] Peng, W., Zhu, J., Huang, M., Lan, Y., Zhao, H., Huang, S., Tang Z. (2024). A bibliometric-based analysis of research progress in unmanned aerial remote sensing of wheat. *INMATEH–Agricultural Engineering*, Vol. 74, pp. 209-217, Bucharest / Romania. https://doi.org/10.35633/inmateh-74-18.

[9] Sun X., Zhang B., Zhang Z., Jing C., Gu L., Zhen W. & Gu X. (2025). Coupling decision of water and nitrogen application in winter wheat via UAV hyperspectral imaging. *Field Crops Research*, Vol. 334, pp. 110159-110159, Elsevier / Netherlands. https://doi.org/10.1016/J.FCR.2025.110159.

[10] Su, X., Nian, Y., Shaghaleh, H., Hamad, A., Yue, H., Zhu, Y., & Hamoud, Y. (2024). Combining features selection strategy and features fusion strategy for SPAD estimation of winter wheat based on UAV multispectral imagery. *Frontiers in Plant Science*, Vol. 15, pp. 1404238-1404238, Frontiers Media S.A. / Switzerland. https://doi.org/10.3389/FPLS.2024.1404238.

[11] Wang, Y., Wu, L., Wei, Z., Tan, T., Yu, Y., Wang, Z., & Huang, K. (2025). Coordinating food security and environmental performance in Belt and Road agrifood systems. *Resources, Conservation&Recycling*, Vol. 219, pp. 108304-108304, Elsevier / Netherlands. https://doi.org/10.1016/J.RESCONREC.202 5.108304.

[12] Wu, Y., Yuan, S., Zhu, J., Tang, Yue. & Tang, Lingdi. (2025). Estimation of Wheat Leaf Water Content Based on UAV Hyper-Spectral Remote Sensing and Machine Learning. *Agriculture*, Vol. 15, pp. 1898-1898, MDPI / Switzerland. https://doi.org/10.3390/AGRICULTURE15171898.

[13] Wang Q., Chen X., Meng H., Miao H., Jiang S, Chang Q. (2023). UAV Hyperspectral Data Combined with Machine Learning for Winter Wheat Canopy SPAD Values Estimation. *Remote Sensing*, Vol. 15, MDPI / Switzerland. https://doi.org/10.3390/RS15194658.

[14] Xian, G., Liu, J., Lin, Y., Li, S., & Bian, C. (2024). Multi-Feature Fusion for Estimating Above-Ground Biomass of Potato by UAV Remote Sensing. *Plants*, Vol. 13, pp. 3356-3356, MDPI / Switzerland. https://doi.org/10.3390/PLANTS13233356.

[15] Xin Y., Rui Y., Yin Y., Ziran Y., Daozhong W., Keke H. (2021). Winter wheat SPAD estimation from UAV hyperspectral data using cluster-regression methods. *International Journal of Applied Earth Observation and Geoinformation*, Vol. 105, Elsevier / Netherlands. https://doi.org/10.1016/J.JAG.2021.102618.

[16] Yang, X., Zhou, H., Li, Q., Fu, X,. & Li, H. (2025). Estimating Canopy Chlorophyll Content of Potato Using Machine Learning and Remote Sensing. *Agriculture*, Vol. 15, pp. 375-375, MDPI / Switzerland. https://doi.org/10.3390/AGRICULTURE15040375.

[17] Yang, S., Li, L., Fei, S., Yang, M., Tao, Z., Meng, Y., & Xiao, Y. (2024). Wheat Yield Prediction Using Machine Learning Method Based on UAV Remote Sensing Data. *Drones*, Vol. 8, pp. 284-284, MDPI / Switzerland. https://doi.org/10.3390/DRONES8070284.

[18] Zhu, J., Zhao, H., Lv, Y., Liang, Z., FU, Y., Liang, Y., & Lan, Y. (2025). Evaluating freeze damage in winter wheat using vegetation index and texture-color features of unmanned aerial vehicle(基于无人机植被指数与纹理-颜色特征融合的冬小麦冻害评价). *Transactions of the Chinese Society of Agricultural Engineering*, Vol. 41, pp. 165-173, Beijing / China. DOI:10.11975/j.issn.1002-6819.2025 03144.

[19] Zhang, C., Yi, Y., Zhang, S., & Li, P. (2024). Quantitative Analysis of Vertical and Temporal Variations in the Chlorophyll Content of Winter Wheat Leaves via Proximal Multispectral Remote Sensing and Deep Transfer Learning. *Agriculture*, Vol.14, pp. 1685-1685, MDPI / Switzerland. https: //doi.org/10.3390/AGRICULTURE14101685.

[20] Zhao J., Li H., Chen C., Pang Y. & Zhu X. (2022). Detection of Water Content in Lettuce Canopies Based on Hyperspectral Imaging Technology under Outdoor Conditions. *Agriculture*, Vol. 12, pp. 1796-1796, MDPI / Switzerland. https://doi.org/10.3390/AGRICULTURE12111796.